The Surface, Interface and Bulk Properties of Advanced Ceramics

Technical Highlights

Sandia National Laboratories
Livermore, CA

Term of review FY99 – FY2001

Contact:Robert Q. Hwang,
Sandia National Laboratories, Livermore, CA 94551
Telephone: (925) 294-1570
Fax: (925) 294-3231
Email: rqhwang@sandia.gov

Sandia National Laboratories

The Surface, Interface, and Bulk Properties of Advanced Ceramics

Kevin F. McCarty
September 2001

Sandia National Laboratories
Livermore, CA

Table of Contents

Abstract

This project focuses upon the science of ceramic surfaces and their interfaces with metals. Our effort includes determining the surface structure of ceramics such as alumina using electron diffraction analysis. In addition, we directly follow the dynamics of surface morphology and structure in real time using the microscopic techniques of scanning tunneling microscopy (STM) and low-energy electron microscopy (LEEM). We strive to quantitatively understand how mass transport occurs on the surface and through the bulk and to characterize the nature and energetics of the bulk thermal defects. We form metal/ceramic interfaces by depositing metals on ceramic single crystals (such as alumina and titanium dioxide) and by oxidizing metal alloys (such as NiAl). We determine how the metals nucleate and grow on ceramic surfaces and the mechanisms of alloy oxidation. We seek to understand how metal/ceramic interfaces evolve during film growth and how interface structure, bonding, and reaction influence the interfacial energy ("strength") and microstructure of the growing film. Through understanding the energetics of metal particles on ceramics, we hope to be able to control the size and morphology of the particles. Our long-range goal is to develop sufficient understanding so ceramic surfaces and their interfaces with metals can be scientifically tailored for improved performance and new properties.

Motivation and Approach

Advanced ceramics and their interfaces with metals play a critical role in many technologies directly related to DOE's missions in Energy, the Environment, and National Security. For example, ceramics are used in high-temperature structural applications (turbines and engines),[1,2] as catalyst supports,[3] sensors,[4-6] and, potentially, as repositories for radioactive waste.[7] Metal/ceramic interfaces are essential for ceramic joining,[8] thermal barrier coatings,[9] metal/ceramic composites,[10,11] supported heterogeneous catalysts,[3] and the electrical interconnects and packaging in microelectronics.[12] These interfaces also greatly influence how metals corrode.[13]

The utility of ceramics and their interfaces with metals is only matched by their complexity. To begin with, ceramics typically have crystal structures that are much more complicated than those of elemental materials and simple compound semiconductors such as GaAs.[14] Because of this complexity, many fairly basic issues regarding ceramics have not been determined.[15] For example, until very recently, the static structure of the simplest surface of α-Al_2O_3 (sapphire) was ambiguous.[16-19] In addition, it is not well understood how the mass transport responsible for the thermal smoothing of a rough surface or the sintering of granular materials occurs.[20,21] The mass transport can occur along the surface and along grain boundaries or, alternatively, through the bulk of the material itself.[22,23] Even for titanium dioxide, one of the most studied non-stoichiometric ceramics, there is ambiguity regarding the nature of the dominant structural and thermal defects.[24] The nature and energetics of bulk structural and thermal defects in ceramics are usually not directly measured. Instead, they are inferred, frequently with ambiguity, from measuring properties like the electrical conductivity as a function of temperature and pressure.[21] Even less studied is the relationship between these bulk defects and mass transport, either on the surface or through the bulk.

The complexity is even greater for metal/ceramic interfaces.[25,26] These interfaces typically involve materials with large differences in properties, for example, an ionically bonded ceramic joined to a metallically bonded metal. Because the materials are dissimilar, new types of bonding across the interface can occur. For example, the formation of image charges across the interface ("polarization") can dominate the interfacial bonding.[25,27] The metal can chemically react with the ceramic, as sometimes desired to produce a stronger interface, or little reaction can occur. The details of the bonding and interfacial reactions can greatly alter the strength.[26] Finally, the pathway through which an interface forms can influence the ultimate properties. For example, how a metal initially nucleates on a ceramic surface can alter the ultimate metal microstructure[28] and thus the mechanical and other physical properties of the structure.[29]

This project focuses on two specific aspects of ceramics -- their surfaces and their interfaces with metals. We determine the surface structure of prototype ceramics such as α-Al_2O_3 using dynamical analysis of low-energy electron diffraction.[19,30] This effort involves a collaboration with Michel Van Hove of the Lawrence Berkeley National Laboratory. As a demanding test of theory, the experimental structures are compared to predictions from state-of-the-art calculations. We also use the surface-imaging technique of low-energy electron microscopy (LEEM) to follow in real time the dynamical processes occurring on ceramic surfaces. The technique generates image contrast between regions having different chemical composition and/or atomic order in the topmost atomic layers.[31] In addition, the technique can readily image the location of surface steps, even those a single atom high; the lateral image

resolution is better than 10 nm. The LEEM instrument is designed to image at variable temperatures and during the growth of surface structures as fluxes impinge on the surface (Fig. 1). By observing step motion, we quantify in real time how the surface morphology changes. We have recently developed a LEEM-based technique capable of determining the type and energetics of bulk defects in materials. In the technique, the sample's temperature is oscillated and the size change of surface features (i.e., changes in island size) is measured.[32] The size changes result from temperature-dependent changes in the bulk defect concentration. As we have demonstrated for the intermetallic alloy NiAl,[32] this technique can also evaluate which mass transport processes control the morphological evolution of the surface. For example, determining whether mass is transported along the surface or through the bulk and determining what ad-species (or bulk defects) are diffusing.

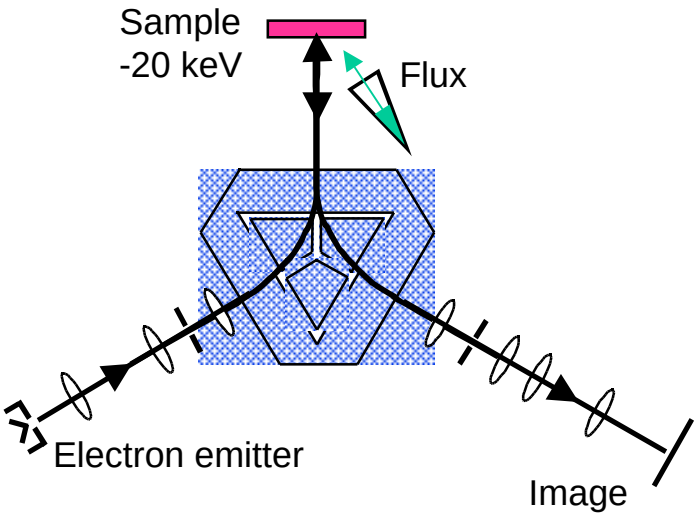

Fig. 1. Schematic illustration of a low-energy-electron microscope (LEEM). Images are formed using electrons reflected from the surface. Contrast comes from surface morphology, crystal structure, and chemical composition. The technique readily images surface steps and their motion.

We prepare metal/ceramic interfaces by either depositing a metal on a ceramic or oxidizing an alloy such as NiAl. We study these processes using scanning tunneling microscopy (STM) and LEEM. The surface morphology of the deposited metal film is followed using STM. This approach directly distinguishes between wetting and non-wetting (three-dimensional) metal-growth mechanisms. For the non-wetting case, the interfacial energy can be determined by measuring the shape of the metal particle.[33] Compared to metal-on-metal growth,[34] the details of metal-on-ceramic growth are poorly understood.[35,36] Incompletely answered questions include: Do islands always nucleate at defects or does homogeneous nucleation also occur? How is the metal deposition flux partitioned between islands? For three-dimensional growth, how do the metal atoms go from the diffusing on the ceramic's surface to being incorporated into a 3D island above the ceramic's surface? How is the strain of lattice mismatch accommodated and what role does stress have in island growth?

Important questions also remain about how a metal alloy oxidizes. For example, oxidation of NiAl can result in formation of spinel ($NiAl_2O_4$) or the more thermodynamically stable phase alumina.[37] But alumina formation requires some process that rejects Ni from the

interface. Recent first-principles calculations suggest that this process occurs by the segregation of Ni vacancies to the surface,[38] but no experimental confirmation exists.

Theory and modeling form an intimate part of this project. These efforts are supported either directly or occur through collaborations. First-principle, electronic-structure techniques are used by Dwight Jennison (Sandia National Laboratories, New Mexico) to compute the atomistic structure and properties (i.e., interfacial energy) of ceramic surfaces and metal/ceramic interfaces. "Mesoscopic-scale" models are developed and applied by Norman Bartelt, Istvan Daruka, and François Léonard (all Sandia National Laboratories, California) to understand the dynamics of ceramic surfaces and their interfaces with metals.

In summary, the first goal of this project is to better understand the inherently complex surface structure of ceramics such as sapphire. We next strive to observe, quantify, and understand the dynamics (e.g., step motion during thermal smoothing) that occur on ceramic surfaces. From this starting point, we then seek to determine how metal/ceramic interfaces evolve during film growth and how interface structure, bonding, and reaction influence the interfacial energy ("strength") and microstructure of the film. We hope to be able to control the size, morphology, and chemical reactivity of metal particles on ceramics by understanding the growth process and energetics.

Facilities

This project enjoys state-of-the-art experimental facilities. Two, independent, ultrahigh-vacuum (UHV) STM systems are dedicated to the effort. These systems are fully equipped with the usual surface-science diagnostics of low-energy electron diffraction (LEED), Auger spectroscopy, ion sputtering, and mass spectroscopy. One of the STM systems has a load-lock assembly for rapid insertion of samples and STM tips. The other STM system was designed for variable-temperature imaging. While this capability is not currently operational, only minor changes are required to enable the variable-temperature imaging. In both systems, the sample can be exposed to a variety of fluxes, including atomic oxygen and metal atoms.

The low-energy electron microscope (LEEM) is shared with the OBES project Science of Materials. This system has a dedicated sample preparation chamber, which will soon have the capability for Auger spectroscopy. A load-lock assembly allows rapid sample insertion from ambient. In addition, the LEEM has a sample storage garage in which five samples can be stored in UHV isolated from the sample preparation and imaging chambers. In addition, we have all the hardware and software needed to digitally capture and analyze the video-rate image stream.

Personnel

Principal Investigator: Kevin F. McCarty

Post-doctoral Researchers:

Curtis F. Walters, 1998-2000. Currently employed at Novellus Systems Inc., San Jose, CA.

Donna A. Chen, 1998-1999. Currently Assistant Professor in the Dept. of Chemistry and Biochemistry, Univ. of South Carolina.

Sean M. Seutter, 1999-2000. Currently employed at Applied Materials Inc., Santa Clara, CA.

Funding Summary

FY98 – 348K FY99 – 317K FY00 – 392K FY01 – 399K

Collaborations and Relationship to Other Projects

This project (The Surface, Interface, and Bulk Properties of Advanced Ceramics, SCW1550) relies on collaborations both internal and external to Sandia National Labs. The effort in surface-structure determination using dynamical low-energy electron diffraction combines our experimental work with the structural simulations performed by Michel Van Hove of the Lawrence Berkeley National Laboratory (LBL). The work on NiAl oxidation was performed in consultation with Peggy Hou, also of LBL.

This project also collaborates extensively with other OBES-sponsored projects at Sandia/California and Sandia/New Mexico. Our work on the surface science of ceramics is very synergist with the effort on metal surfaces and metal films occurring within the Sandia/California project on the Science of Materials (SCW0604). Experimental collaborations at Sandia/California include those with Douglas Medlin (SCW0604). Using transmission electron microscopy techniques, he has examined the structure of the metal/ceramic interfaces synthesized in this project. The Advanced Ceramics project also benefits greatly from the computational material science efforts occurring within the Science of Materials project. Specifically, an important focus of the Advanced Ceramics project is measuring the dynamics of ceramic surfaces and metal/ceramic interface formation. The approach of Norman Bartelt and his colleagues is to write down the equations of motion controlling the dynamics. This powerful approach allows the experimental observations to be directly modeled. In this manner, the dominant processes can be determined and the fundamental quantities (e.g., rates and energies) governing the dynamics can be extracted. In addition, Istvan Daruka is contributing to the NiAl oxidation effort by developing a detailed kinetic model of the anisotropic island growth.

Finally, we team with Dwight Jennison, who is supported by the OBES/Material Science program of Sandia/New Mexico. He uses first-principle, electronic-structure techniques to compute the atomistic structure and properties (i.e., interfacial energy) of the ceramic surfaces and the metal/ceramic interfaces that we study experimentally. Combining these simulations with experimental determinations of structure is a powerful approach.

Publications

K. F. McCarty, J. A. Nobel, and N. C. Bartelt, “Vacancies in Solids and the Stability of Surface Morphology,” Nature **412** 622(2001).

E. A. Soares, M. A. Van Hove, C. F. Walters, and K. F. McCarty, "The Structure of the α-Al_2O_3 (0001) Surface from Low-Energy Electron Diffraction: Al Termination and Evidence for Anomolously Large Thermal Vibrations," submitted to Phys. Rev. B (2001).

K. F. McCarty, “Imaging the Crystallization and Growth of Oxide Domains on the NiAl (110) Surface,” Surf. Sci. **474** L165 (2001).

C. F. Walters, K. F. McCarty, E. A. Soares, and M. A. Van Hove, “The Surface Structure of α-Al_2O_3 Determined by Low-Energy Electron Diffraction: Aluminum Termination and Evidence for Anomolously Large Thermal Vibrations,” Surf. Sci. **464**, L732 (2000).

D. A. Chen, M. C. Bartelt, S. M. Seutter, and K. F. McCarty, "Small, Uniform, and Thermally Stable Silver Particles on TiO_2 (110)-(1×1)," Surf. Sci. **464**, L708 (2000).

D. A. Chen, M. C. Bartelt, R. Q. Hwang, and K. F. McCarty, “Self-Limiting Growth of Copper Islands on TiO_2 (110),” Surf. Sci. **450** 78 (2000).

K. F. McCarty, “Preferred Orientation in Carbon and Boron Nitride -- Does a Thermodynamic Theory of Elastic Strain Energy Get It Right?,” J. Vac. Sci. Technol. A **17** 2749 (1999).

J. R. Heffelfinger, D. L. Medlin, and K. F. McCarty, “On the Initial Stages of AlN Thin-Film Growth onto (0001) oriented Al_2O_3 Substrates by Molecular Beam Epitaxy,” J. Appl. Physics **85** 466 (1999).

J. R. Heffelfinger, D. L. Medlin, and K. F. McCarty, "Epitaxy of AlN (Wurtzite Structure) Thin Films Grown on MgO (Rock-Salt Structure),” J. Mater. Res. **13** 1414 (1998).

Invited Talks

K. F. McCarty, J. A. Nobel, N. C. Bartelt, “Dynamics on the Clean and Oxidized NiAl Alloy Surface,” American Vacuum Society Meeting, San Francisco, CA, Oct. 2001.

K. F. McCarty, J. A. Nobel, N. C. Bartelt, “The role of bulk vacancies on the surface dynamics of NiAl and TiO_2,” American Chemical Society Meeting, Orlando, FL, Apr. 2002.

Overview of past work

About three years ago, the emphasis of this project was switched from studying the synthesis of nitride thin films (boron nitride and aluminum nitride) to oxide surfaces and their interfaces with metals.

The significant accomplishments of this project over the past 3 years include:

- Discovered the "self-limiting" growth of Cu and Ag particles on the TiO_2 (110) surface.
  D. A. Chen, M. C. Bartelt, R. Q. Hwang, and K. F. McCarty, "Self-Limiting Growth of Copper Islands on TiO_2 (110)," Surf. Sci. **450** 78 (2000).

- Determined the structure of the α-Al_2O_3 (0001) surface.
  C. F. Walters, K. F. McCarty, E. A. Soares, and M. A. Van Hove, "The Surface Structure of α-Al_2O_3 Determined by Low-Energy Electron Diffraction: Aluminum Termination and Evidence for Anomolously Large Thermal Vibrations," Surf. Sci. **464**, L732 (2000).

  E. A. Soares, M. A. Van Hove, C. F. Walters, and K. F. McCarty, "The Structure of the α-Al_2O_3 (0001) Surface from Low-Energy Electron Diffraction: Al Termination and Evidence for Anomolously Large Thermal Vibrations," submitted to Phys. Rev. B (2001).

- Developed a new technique to determine the nature and energetics of bulk defects.
  K. F. McCarty, J. A. Nobel, and N. C. Bartelt, "Vacancies in Solids and the Stability of Surface Morphology," Nature **412** 622(2001).

- Showed that bulk diffusion (rather than surface diffusion) can dominate the morphological evolution of a surface.
  K. F. McCarty, J. A. Nobel, and N. C. Bartelt, "Vacancies in Solids and the Stability of Surface Morphology," Nature **412** 622(2001).

- Observed how a binary alloy oxidizes to form alumina.
  K. F. McCarty, "Imaging the Crystallization and Growth of Oxide Domains on the NiAl (110) Surface," Surf. Sci. **474** L165 (2001).

A detailed description of these accomplishments is given below. Full details are contained in the literature publications.

Discovery of Self-Limiting Growth During Metal/Ceramic Interface Formation

D. A. Chen, M. C. Bartelt, R. Q. Hwang, and K. F. McCarty
Sandia National Laboratories, Livermore, CA 94551

Motivation:

To better understand how metal/ceramic interfaces form, evolve, and affect ultimate system performance, we have studied how metals (copper and silver) grow on a model ceramic (rutile) under well-characterized conditions.[39,40]

Accomplishment:

The rutile (110) surface consisted of atomically flat terraces about 100 Å in width separated by unit-cell-high steps. The nucleation of copper and silver on rutile (TiO_2) was studied using scanning tunneling microscopy (STM) under ultrahigh vacuum conditions. The resulting metal islands nucleated preferentially at step edges and grew in three dimensions (3D). That is, rather than growing laterally and covering the substrate (i.e., 2D growth), the Cu and Ag islands grow up, forming islands with high aspect ratios (see Fig. 2). Computer simulations showed that the observed 3D islands can only form if there is an "upflow" of deposited metal atoms from the rutile surface onto the islands. A striking behavior was discovered in the dependence of island size and density on metal dose -- namely, the metal islands grow to a temperature-dependent size and then essentially stop growing. Additional metal dosing produces new islands (i.e., additional nucleation), but not larger particles. This behavior is in marked contrast to conventional film growth (e.g., formation of metal/metal interfaces), for which increased deposition results in island growth and no addition nucleation.

The Ag and Cu islands were remarkably stable under thermal annealing -- long-term or high-temperature anneals increased the island diameter by less than a factor of two. The observation that metal adatoms on average diffuse across a terrace width before being captured by an island allows us to give lower bounds for the metal diffusion rates on TiO_2 (110). Ag, adatoms diffuse at $>10^{-9}$ cm^2/s compared to at least 10^{-10} cm^2/s for Cu adatoms. Finally, the work of adhesion (W_{ad}) was determined by measuring the particle shapes. The Ag/TiO_2, interface (W_{ad} = 1.4 J/m^2) is weaker than the Cu/TiO_2, interface (W_{ad} = 2.4 J/m^2). This trend, as well as that of the diffusion rates, is consistent with Ag having a lower oxygen affinity and lower heat of oxide formation than Cu.

Significance:

Scientifically, our findings establish a new mechanism of interface formation that occurs because of the greatly differing properties of the metal and ceramic. Because the metal interacts weakly with the ionic substrate and prefers to bond to itself, the deposited metal diffuses from the substrate onto the metal islands, giving 3D growth. But the "upflow" process stops when the metal particle reaches a critical size, producing a unique self-limiting growth. Technologically, our discovery has impact in two broad areas. First, self-limiting growth may be the underlying mechanism controlling grain structure in metal films on ceramics. That is, the process limits the island size, which in turn sets the length scale of grains in the resulting film. Second, our discovery offers a way to make metal particles with a narrow size distribution. The particle size can be altered simply by changing the deposition temperature. Narrow sizes are desired for technologies such as quantum-dot electronics, chemical sensors, and catalysts.

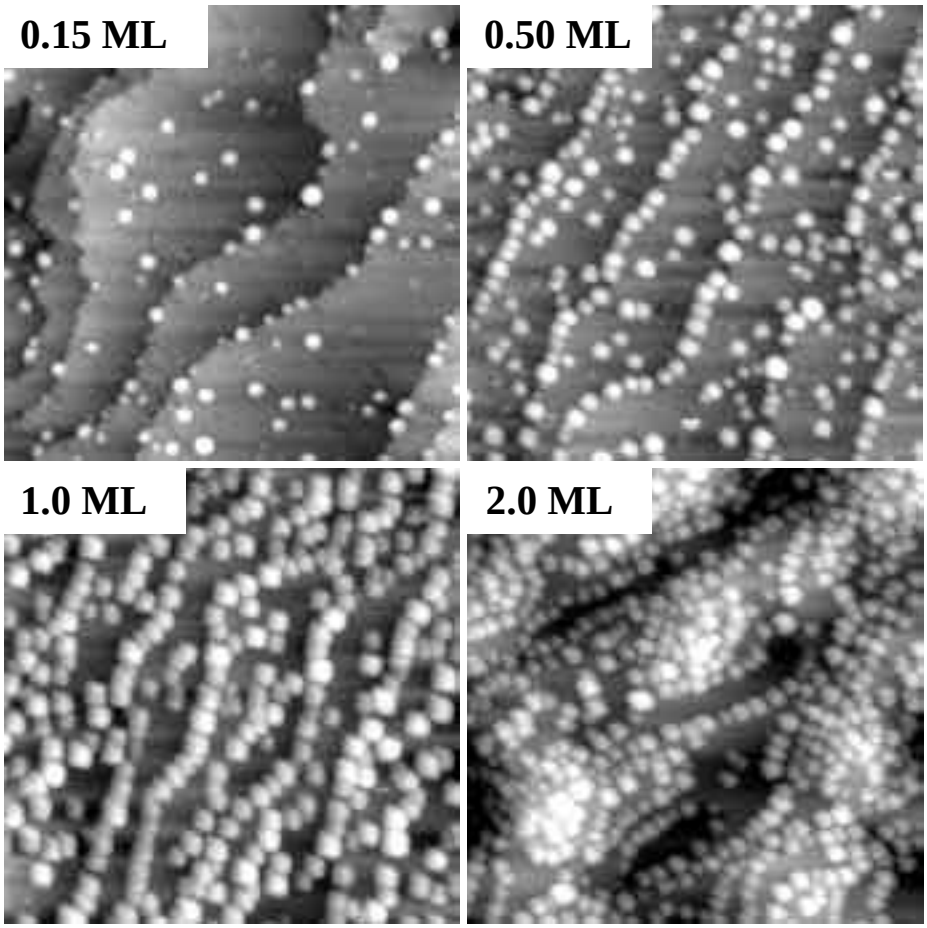

Fig. 2. STM images (1000 x 1000 Å^2) of a rutile (110) surface dosed with between 0.5 and 2.0 monolayers of Cu. With increased dose, the Cu particles hardly increase in size but the number of particles increases greatly.

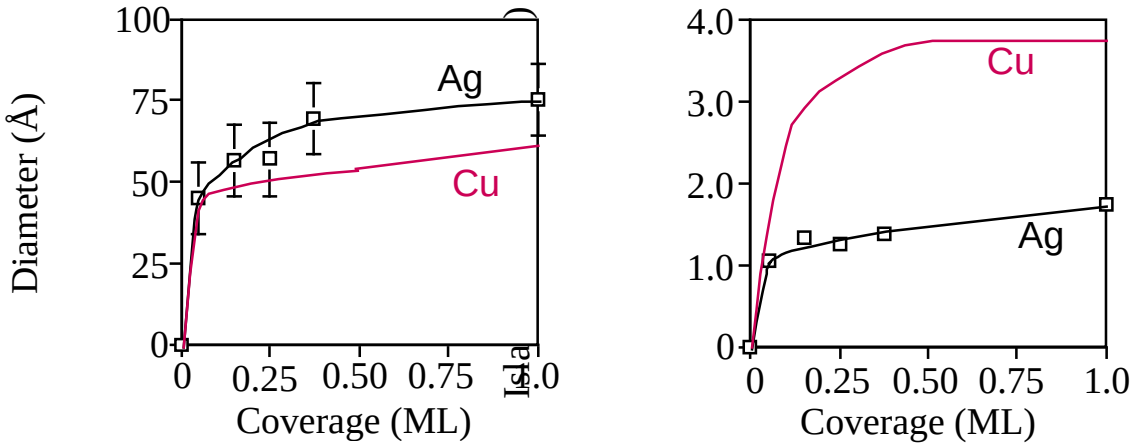

Fig. 3. Plot showing that the size of Cu and Ag islands grown at room temperature on TiO_2 "self-limit." That is, the diameter saturates.

Determination of the Surface Structure of α-Al_2O_3 (0001)

C. F. Walters,[1] K. F. McCarty,[1] E. A. Soares,[2] and M. A. Van Hove[2]

[1]Sandia National Laboratories, Livermore, CA 94551
[2]Lawrence Berkeley National Laboratory, Berkeley, CA 94720

Motivation:

Being the simplest and the only thermodynamically stable aluminum oxide, α-Al_2O_3 is a prototype for understanding metal oxides.[41] Because of this importance, sapphire surfaces have been extensively studied by experiment and theory. Nonetheless, a most basic property of its simplest clean surface, namely the structure of α-Al_2O_3 (0001), remains controversial.[19,42]

Determining the surface structure of a compound such as alumina is much more complicated than for a mono-atomic material. First, the (0001) surface can terminate in a single Al layer, an oxygen layer, or a double Al layer (Fig. 4). In addition, the stacking periodicity at the surface may differ from that of the bulk. Finally, compound surfaces can potentially be phase-separated, i.e., consist of coexisting terraces having different stoichiometry or structure. The existence of a phase-separated surface may depend sensitively on processing conditions. Therefore, we have studied the α-Al_2O_3 (0001) surface with particular emphasis on two issues – sensitivity to sample preparation and completeness of analysis.

Accomplishment:

Using dynamical low-energy electron diffraction,[30] we have determined the structure of the α-Al_2O_3 (0001) surface. The diffraction results for 3 different preparations were analyzed using an exhaustive search of possible models, which included different terminations, mixtures of terminations, and stacking faults.

We conclude that the surface termination of α-Al_2O_3 (0001) is a single Al layer, that the first interlayer spacing is significantly contracted with respect to the bulk spacing, and that the surface structure is insensitive to our different processing methods (Fig. 5). In addition, we have determined that the topmost Al atoms have unusually large vibrational amplitudes at room temperature.

Significance:

We have resolved the contradictory experimental results regarding the termination of α-Al_2O_3 (0001). More importantly, we provide the first experimental evidence for enhanced vibrations at an oxide surface. Such vibrations account for the substantial difference between the interlayer contractions determined by zero-temperature calculations and finite-temperature experiments. These large vibrations will have important implications for both the structural and chemical properties of alumina and other oxides and highlight the limitations of even state-of-the-art computations.

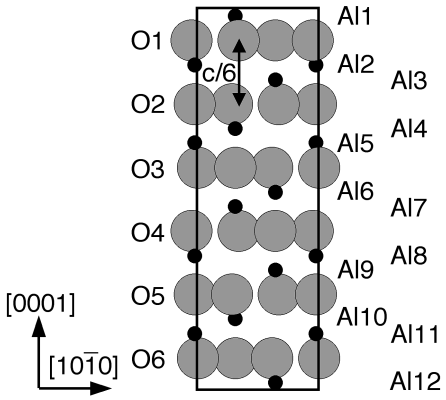

Fig. 4. Illustration of the 12 Al layers and 6 O layers, parallel to the (0001) surface, of the sapphire unit cell. The surface can be terminated by a single Al layer (i.e., Al1), an oxygen layer (O1), or a double Al layer (Al2+Al3).

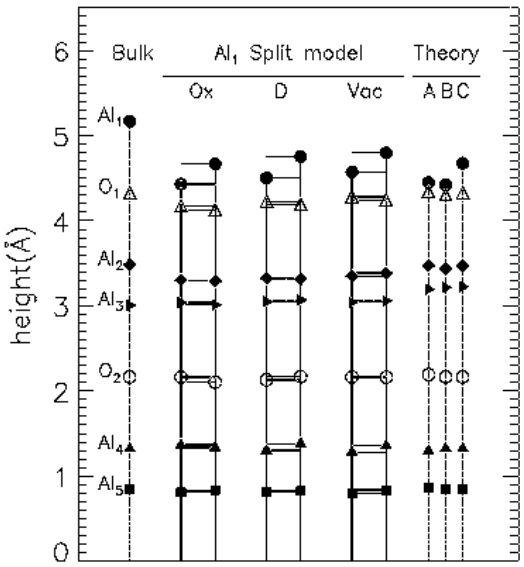

Fig. 5. Graphical representation of the atomic positions perpendicular to the α-Al_2O_3 (0001) surface, for 3 different sample preparations, compared to bulk and theory. Because of the large vibrational amplitude of the topmost Al atoms, the surface must be modeled using the "split-position" method. Physically, however, the Al atoms are at the average position. State-of-the art theory only models the system at zero temperature. Because of the anharmonic surface vibrations, significant expansion occurs at room temperature. Thus the theory overestimates the contraction of the outermost layer.[43]

Bulk Vacancies are Created at Surface Steps

K. F. McCarty, J. A. Nobel, and N. C. Bartelt
Sandia National Laboratories, Livermore, CA 94551

Motivation:

Since thermally generated vacancies in solids are known to control many materials properties (e.g., solid-state diffusion), it is important to understand how thermal vacancies are created and destroyed. Where and how vacancies on surfaces are generated has not been directly established. For example, it is unknown whether bulk vacancies are created over the entire area of a surface, or only at selected sites, such as surface steps.

Accomplishment:

We have used low-energy-electron microscopy (LEEM) to study in real time vacancy generation on the (110) surface of the intermetallic alloy NiAl.[32] We oscillate the sample's temperature and observe the response of the nanoscale surface structure as a function of frequency (a version of Ångström's method of measuring thermal conductivity).[44] We find that vacancies are generated (and annihilated) not over the entire surface, but only near atomic steps (see Fig. 6 and Movie 1 on accompanying CD).

Significance:

To our knowledge, this is the first direct demonstration of where bulk vacancies are formed at a surface. That vacancies on the NiAl (110) surface are generated and annihilated only near the step edges undoubtedly affects how other processes involving vacancies (e.g., surface oxidation) actually occur. We have also demonstrated a new and powerful way to measure important properties of bulk materials. We use the technique to explicitly determine the migration and formation energies of the bulk defects in NiAl.[45] More importantly, we demonstrate that our technique can be used to unambiguously determine the thermal-defect type as a function of temperature and composition.

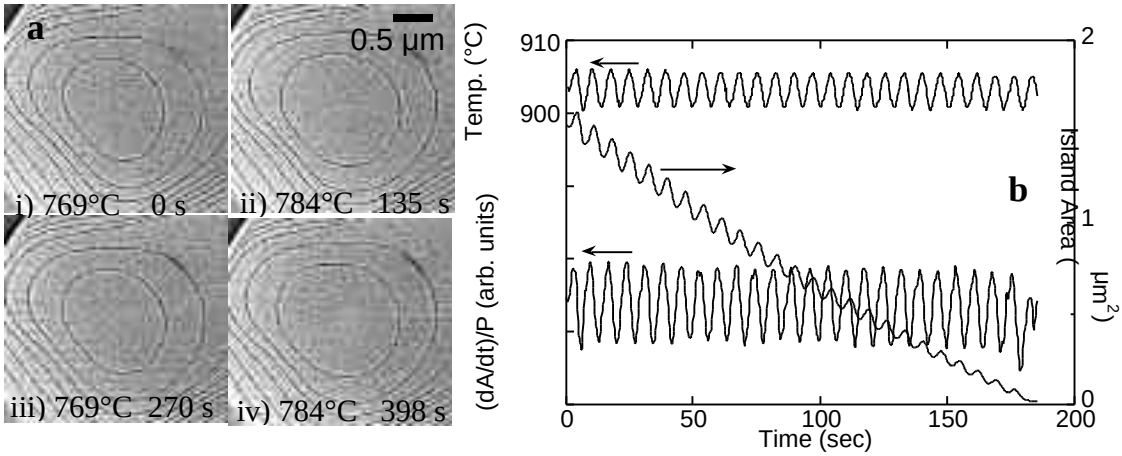

Fig. 6. a) LEEM micrographs of an island-stack structure on the NiAl (110) surface as the temperature is varied about a mean of 776°C. (See Movie 1on accompanying CD). The dark lines mark the atom-high surface steps. With increasing temperature, bulk atoms come to surface since the concentration of thermal vacancies in the bulk increases. For decreasing temperature, the islands shrink in size because material leaves the surface to reduce the bulk vacancy concentration. b) Island area $A(t)$ and the rate of change normalized by the perimeter $(dA/dt)/P$ as the temperature is a sinusoidally oscillated by about ±2.5°C around a mean of 903°C. Even though the island area decreases greatly because of thermal smoothing, the area change resulting from the temperature oscillation scales exactly as the perimeter of the island.

Surface Smoothing Controlled by Bulk (Not Surface) Diffusion

K. F. McCarty, J. A. Nobel, and N. C. Bartelt
Sandia National Laboratories, Livermore, CA 94551

Motivation:

Understanding the mechanisms through which mass diffuses on surfaces and through the bulk is key to the ability to fabricate engineered materials and nanoscale structures. The processes that control evolution of surface morphology are almost always viewed as occurring in the topmost one or two surface layers. Here we investigated mass transport on the prototypical intermetallic alloy, NiAl, without ambiguity, using a new microscopic technique.[32]

Accomplishment:

We measured the thermal smoothing of NiAl (110) by directly observing step motion in real time using low-energy electron microscopy. Remarkably, the decay rates of all islands in a stack (see Fig. 7 and Movie 2 on accompanying CD) are constant in time and totally independent of the local environment (e.g., the width of the immediately adjacent terraces or the size of nearby islands). Given the lack of any surface current between islands of different curvature, we know that surface diffusion is not important to the smoothing process. Instead, we find striking evidence that bulk vacancies are responsible -- we directly observe exchange between bulk vacancies and the surface when the sample temperature is changed (see previous page). The linear-decay kinetics are also consistent with bulk-dominated diffusion. Thus, we conclude that the atoms at surface steps undergo direct exchange with bulk vacancies. Since the steps are interacting directly with the bulk, the surface dynamics are independent of the local environment (i.e., step density and curvature).

Significance:

Our finding that surface smoothing can be dominated by transport through the bulk confirms the mechanism proposed nearly fifty years ago by Herring[22] and Mullins.[23] However, current conventional wisdom is that surface diffusion dominates surface smoothing. We expect similar behavior will be directly observed on other alloys and elemental metals. Because bulk vacancies have larger formation and diffusion activation energies than surface vacancies, bulk processes should become more important at sufficiently high temperature. Our observation has important consequences for the stability of fabricated nanoscale structures.

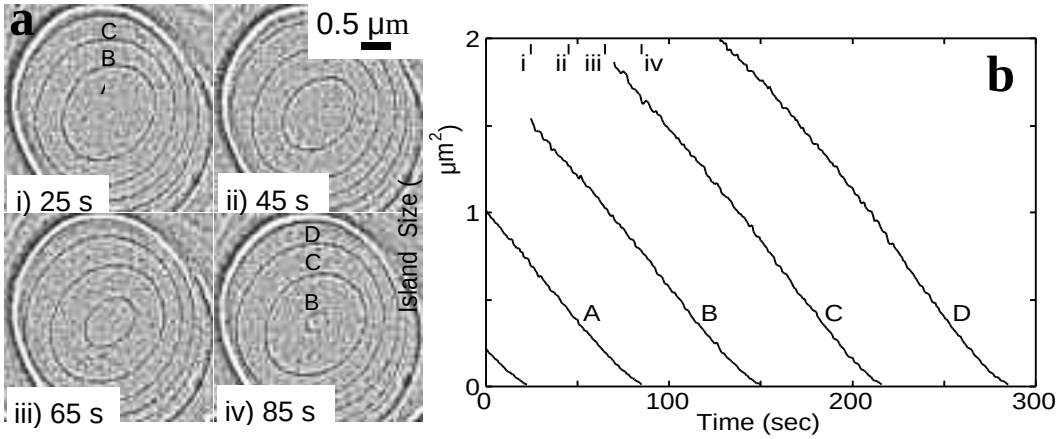

Fig. 7. Smoothing of the NiAl (110) surface. a) LEEM micrographs captured during the constant-temperature decay of an island-stack structure at 957°C. (See Movie 2 on accompanying CD.) The dark lines are the monoatomic surface steps. b) Sizes (square of the largest dimension) of the islands labeled in part a) versus time. Despite the large changes in the local step environment and even though the islands have different curvatures, the islands all decay at the same, constant rate.

Imaging the Oxidation of the NiAl (110) Surface

K. F. McCarty
Sandia National Laboratories, Livermore, CA 94551

Motivation:

One method of making metal/ceramic interfaces is by oxidizing a metal alloy.[46,47] In particular, a procedure to make thin, uniform films of crystalline alumina has been developed based upon oxidizing the (110) surface of the ordered intermetallic alloy NiAl. Here we use real-time microscopy to reveal how the oxide nucleates and grows.[48]

Accomplishment:

We have used low-energy electron microscopy (LEEM) to selectively image the different surface phases that form as the NiAl (110) surface undergoes oxidation. The clean surface was exposed to O_2 at 325°C and then imaged at progressively higher temperatures. While a relatively uniform film results, oxide-free regions (pinholes) develop when the initially amorphous oxide crystallizes. This oxide film consists of one type of alumina that has two orientational domains on the substrate. Selective imaging of the domains just after crystallization shows that nuclei of both domains are present at high density. With time and temperature, the domains coarsen greatly, as do the oxide-free regions (pinholes). (See Fig. 8.) By reducing the length of the domain boundaries, the coarsening reduces the energy.

Significance:

Metal/oxide interfaces are important for ceramic joining, electrical interconnects in microelectronics, supported catalysts, and chemical sensors. For the first time, we have shown that phase-specific imaging of an alloy's surface can be performed in real time as a metal/ceramic interface forms. We directly observe how nucleation and growth occurs and find, unexpectedly, that pinholes develop when the oxide crystallizes.

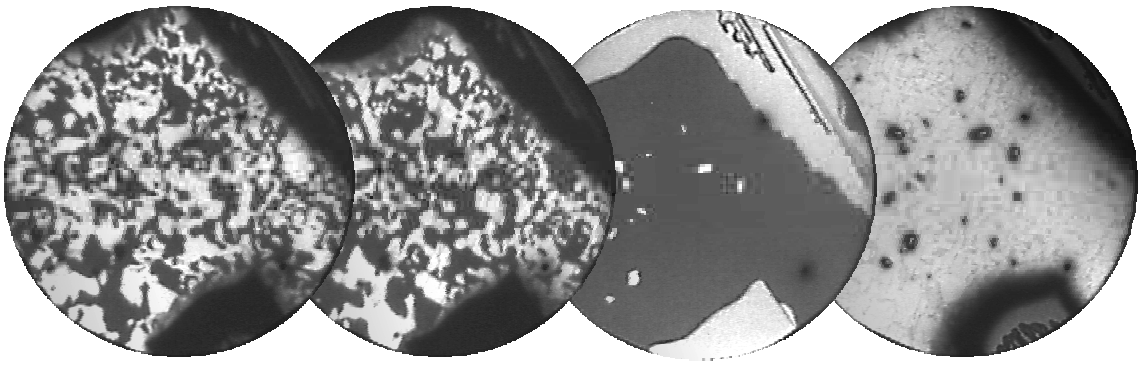

i) DF-1 ii) DF-2 iii) DF-NiAl iv) BF

Fig. 8. LEEM images obtained at 1015°C (5 μm field of view). In images i) and ii), the bright regions correspond selectively to one of the two oxide domains. However, the bright areas in image iii) are regions of bare substrate, showing that the surface is not completely covered with oxide. In the bright-field image (iv), these regions of un-oxidized NiAl substrate appear as dark spots.

Proposed Work

We propose to continue our emphasis on the two closely related topics of 1) the dynamics of oxide surfaces and 2) the dynamics of metal/ceramic interface formation.

Dynamics of oxide surfaces

The mechanisms through which the morphology of oxide surfaces change with time are poorly understood compared to simpler materials. While detailed mechanistic knowledge exists for elemental metals and semiconductors and a few compounds (e.g., GaAs),[49] this is not the case for metal oxides. Consider the case of titanium dioxide (rutile structure), one of the most studied transition-metal-oxide surfaces.[15] Basic questions are how the surface of TiO_2 evolves when annealed and through what processes the morphological evolution occurs. The knowledge is scant and sometimes contradictory. Kitazawa et al. have studied the decay of sinusoidal surface profiles on TiO_2 in air [50] and found the decay rate was proportional to the 2.75 power of the wavelength. Since bulk diffusion should have a dependence of wavelength to the 3.0 power,[23] this work suggests bulk diffusion dominates. They further suggested that Ti diffusion in the bulk was the rate-limiting step. In contrast, Grossmann and Piercy studied the smoothing in vacuum of sputtered TiO_2 (110) using high-resolution electron diffraction. Based on their observation that the average terrace size increased as time to the 4.0 power, they concluded that smoothing was dominated by surface diffusion.

Although still a subject of debate, the dominant defects in TiO_2 are believed to be titanium interstitials and oxygen vacancies.[51] How these bulk defects influence the morphological evolution of a TiO_2 surface is little understood. Vacuum annealing of oxygen-deficient surfaces, prepared by ion sputtering, is known to restore the stoichiometry by diffusion of Ti from the surface to the bulk.[51] Annealing of TiO_2 in oxygen leads to growth of oxide at the surface through reaction of gas-phase oxygen with Ti diffusing (presumably as interstitials) from the bulk.[52] Oxygen annealing at roughly 750°C and below, surprisingly, grows Ti-rich material (near Ti_2O_3 in stoichiometry). The literature contains no explanation for how an oxygen-rich environment results in an oxygen-deficient phase.

We have recently developed the ability to prepare TiO_2 (110) surfaces whose steps are readily imaged in the LEEM. We have already observed that the surface morphology exhibits remarkable behavior with time. We see, for example, that the steps move markedly when the temperature is changed (see Fig. 9), as we previously discovered for NiAl.[32] When the temperature is changed, the concentration of bulk defects changes. The size change occurs because the bulk thermal defects undergo exchange with the surface to equilibrate the bulk. The "sense" of the size change in TiO_2 (steps advance for a temperature increase and retract for a temperature decrease) directly shows that oxygen vacancies are the dominant bulk thermal defect. This is surprising in that the literature usually assumes that titanium interstitials dominate.[51] We have also been able to directly observe step motion during thermal smoothing in vacuum -- an island's step retracts and the island shrinks. Consistently, a pit's step advances and the pit fills in (see Fig. 10). In an oxygen background (see Fig. 11 and Movie 3 on accompanying CD), however, an island's step advances (e.g., island enlarge). This motion occurs as titanium from the bulk reacts with the atmospheric oxygen, causing the surface features to grow in size.[52]

We will quantify the step motion in vacuum and in oxygen environments under isothermal conditions. In addition, we will quantify how surface steps move with temperature changes. We shall develop mathematical models that describe the relationship between mass transport (both on the surface and through the bulk) and step motion. This approach should allow us to determine, for example, if bulk diffusion, surface diffusion, or some combination thereof controls the morphological evolution. As we have done for NiAl, we hope to identify the nature of the bulk defects, their energetics, and their relationship to mass transport, either on the surface or through the bulk.

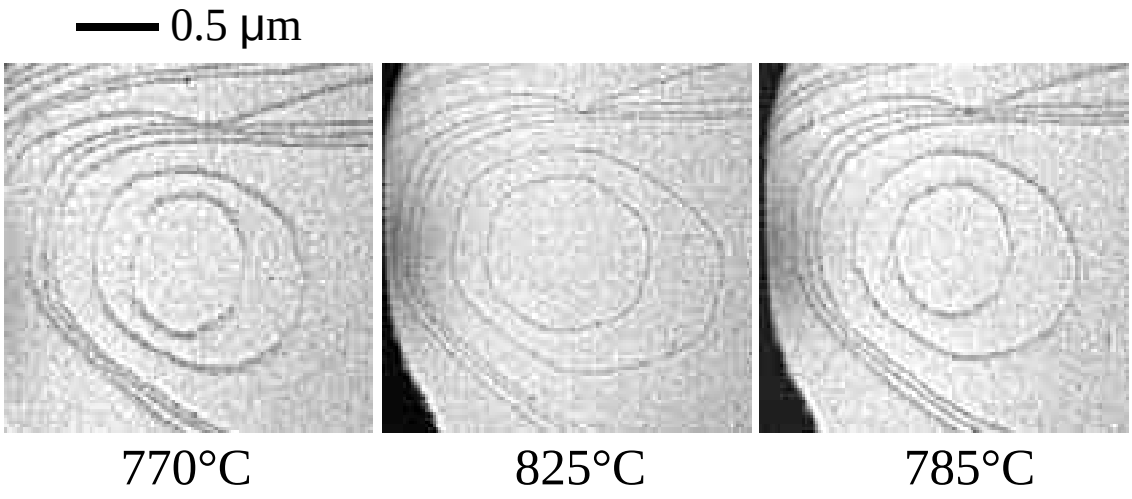

Fig. 9. Temperature-dependent size changes of islands on the TiO_2 (110) surface. When the temperature was increased from 770°C (left image) to 825°C (center image), the two islands enlarge because the concentration of bulk thermal defects increases. The islands shrink when the temperature was reduced to 785°C (right image), showing that the mass transport between the surface and the bulk is reversible.

While the ideal rutile structure has a Ti:O ratio of 1:2, titanium dioxide can accommodate a range of oxygen deficiency, i.e., TiO_{2-x}. If the oxygen deficiency is too great, however, rutile transforms progressively into a series of suboxides, the Magnéli phases of formula Ti_nO_{2n-1}.[53] In fact, titanium dioxide is a prototypical non-stoichiometric ceramic. Understanding transport and how the phase transformations occur in these technologically important materials is a large scientific challenge.[54]

Important aspects of the transformation to the suboxides and bulk transport can be studied by a surface-imaging microscopy technique such as LEEM. Specifically, as rutile becomes more oxygen deficient, the (110) surface undergoes a phase transformation and reconstructs to a structure with (1x2) (lower) symmetry.[55-59] The (1x2) surface is enriched in Ti compared to the un-reconstructed (1x1) surface. Recently, we have been able to observe directly this transformation and have found that it occurs through a surprising pathway (see Fig. 12 and Movie 4 on accompanying CD). Namely, the transformation occurs when the temperature is reduced below a critical value. This critical temperature increases with increasing oxygen deficiency. Consider a (1x1) (un-reconstructed) surface above the critical temperature. As temperature is lowered, steps retract as the concentration of oxygen vacancies in the bulk decreases. At the critical temperature, apparently, the bulk cannot accommodate all the Ti

liberated by the retracting step. The step continues to retract but Ti-rich (1x2)-structure is left in its track. By analyzing this process both experimentally and using the above mentioned mass-transport models, we will develop a detailed picture of the phase transformation.

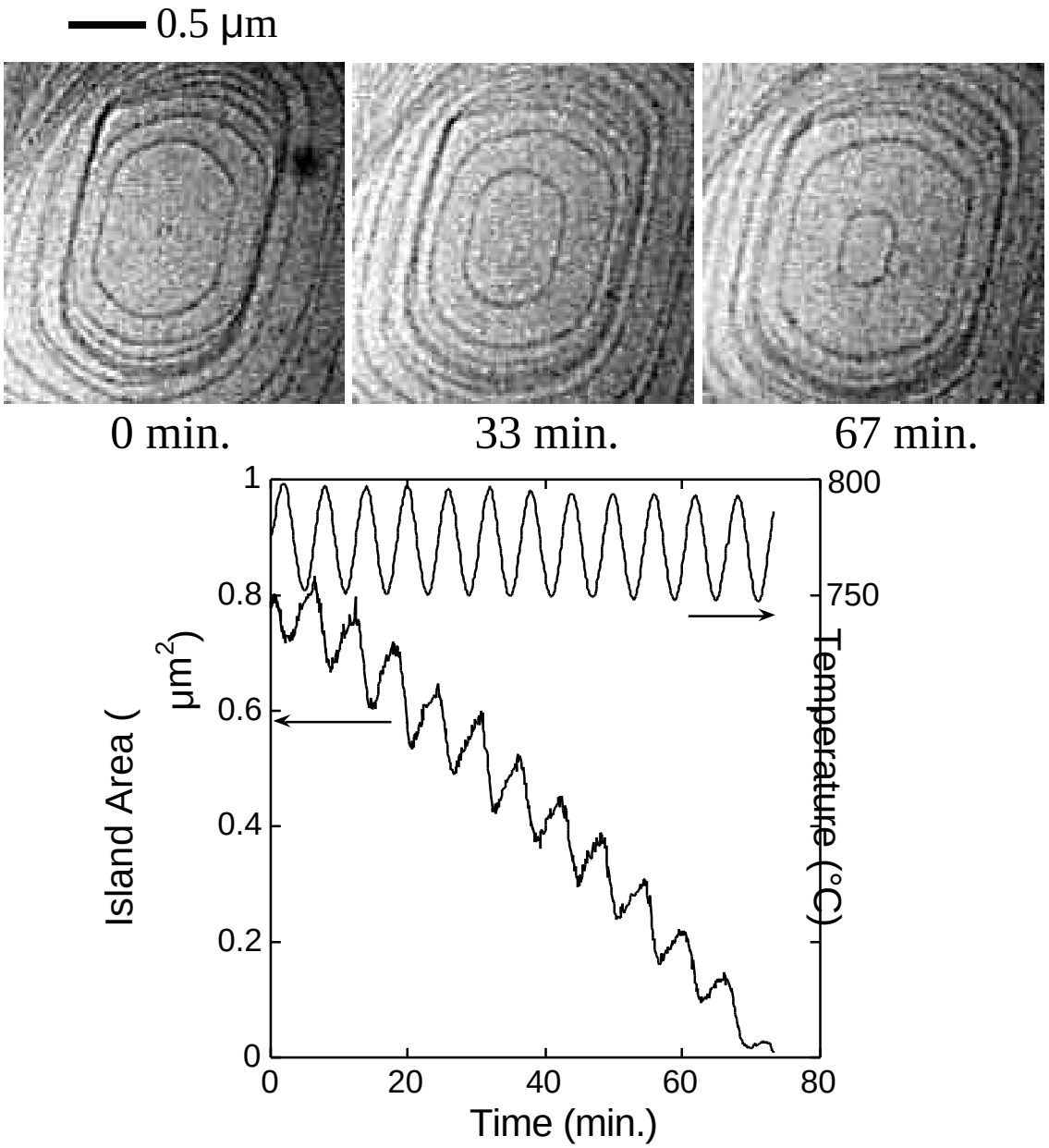

Fig. 10. Thermal smoothing on the TiO_2 (110) surface at about 775°C. The images show that the size of a pit (i.e., a "vacancy island") decreases with time. The sample's temperature was oscillated by about ±20°C during the island decay, causing the island area to also oscillate. Because the feature monitored is a pit, the area change is nearly out-of-phase with the temperature change (i.e., the pit shrinks when the temperature increases and grows when the temperature decreases). Since diffusion is slow relative to the rate of temperature change, there is a phase lag between the temperature and island area. That is, the pit continues to grow after the temperature has started to increase.[32]

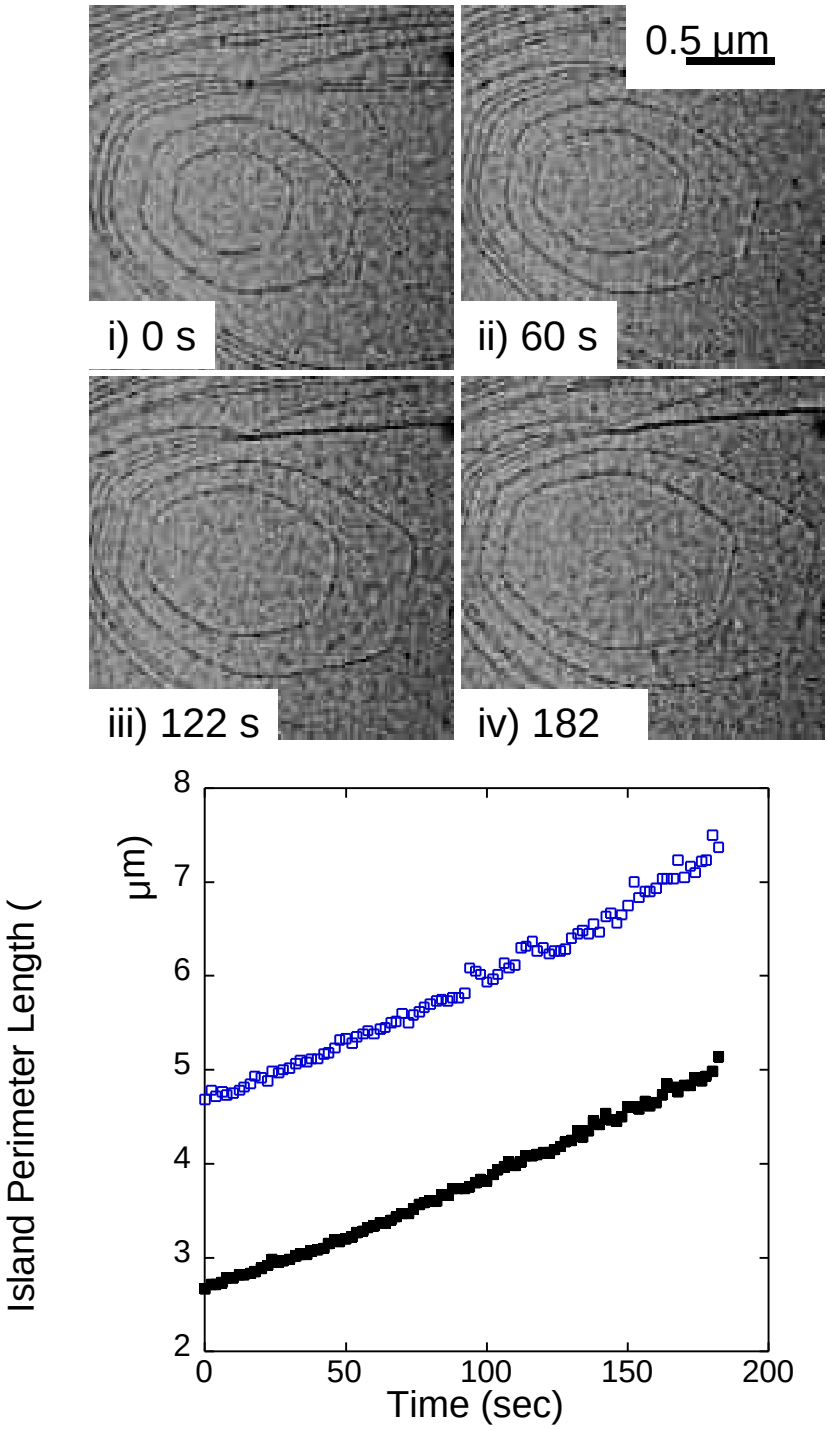

Fig. 11. Island growth on TiO_2 (110) upon exposure to 10^{-6} torr of O_2 at elevated temperature. In the LEEM images, the dark lines mark the surface steps. (See Movie 3 on accompanying CD.) The plot shows that the perimeters (i.e., step length) of the two islands increase at the same and essentially constant rate. This powerful result shows that island growth scales with the perimeter of the islands and suggests that some step-attachment process controls the rate.

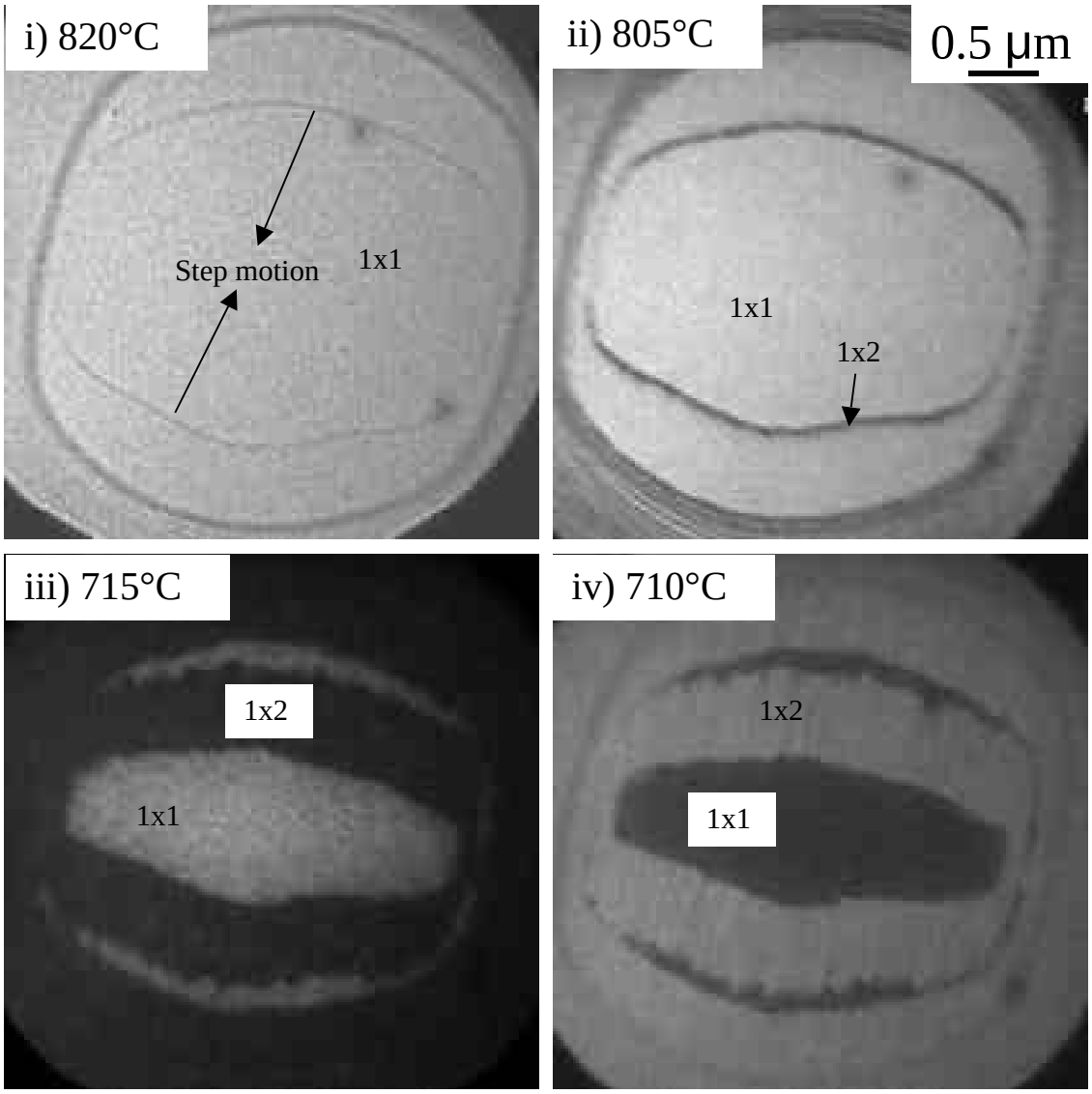

Fig. 12. How the (1x2) structure forms on the TiO_2 (110) surface when the temperature is lowered. (See Movie 4 on accompanying CD.) Images i-iii were obtained in bright field using an electron energy that gives a large contrast between the (1x1) and the (1x2) phases, with the latter phase appearing dark. As the temperature is lowered, the step marked by the arrows in image i retracts (i.e., the island shrinks). If the temperature is above some critical temperature, (1x1) phase is left in the region the step passes through. Below the composition-dependent critical temperature, however, the bulk cannot accommodate all the Ti liberated when the step retracts. Then Ti-rich (1x2) phase is left in the region the step passes through (see images ii and iii). This process can result in complete conversion of a (1x1) surface to a (1x2) surface. The process is essentially reversible – when steps advance upon heating, (1x2) material is converted to 1x1 material. Image iv was obtained in dark field using a diffraction spot unique to the (1x2) phase. That is, in this image, the (1x2) regions are bright while the (1x1) regions are dark, the reversed contrast of the bright-field images.

Dynamics of metal/ceramic interface formation

We will also continue our investigation of the dynamics occurring during metal/ceramic interface formation. We have recently developed the ability to image with STM the exact same region as a metal is deposited onto a ceramic surface. We will use this capability to determine where metal nucleation occurs and to quantify how individual particles grow in their own local environment. This experimental approach, when combined with modeling, has been used in metal-on-metal film studies to determine the controlling processes (e.g., defect vs. homogeneous nucleation, how the deposition flux is partitioned between neighboring islands, etc.).[60] Our initial results for Cu on TiO_2 show that while the initial islands nucleate at preexisting defects on the surface (see Fig. 13),[61] homogeneous nucleation (i.e., on a terrace and not near a preexisting defect) can occur at later stages of growth. Most importantly, by tracking individual islands as a function of metal fluence, we found that the islands saturated in size (height and diameter) even at extremely low copper coverages (see Fig. 14). This indeed establishes that the Cu islands individually self-limit their growth.

We will also use LEEM to study metal/ceramic interface formation. While Cu and Ag islands deposited at room temperature on TiO_2 are too small to be seen in LEEM, we will study the dewetting of films thick enough for island coalesce to have occurred.[62] Figs. 15 and 16 shows the dewetting of Cu films initially about 10Å-thick. We have already observed that the dewetting process depends greatly on the state of the surface. For example, on a (1x1) non-reconstructed surface, relatively isotropic islands result from dewetting (see Fig. 15). Prolonged annealing caused the metal islands to evaporate from the surface. In contrast, on a (1x2) reconstructed surface, dewetting produces very elongated structures (see Fig. 16 and Movie 5 on accompanying CD). The substrate was observed to encapsulate these islands upon prolonged annealing. Such encapsulation has been termed the "strong-metal-support interaction."[15,63] We intend to quantify the dewetting kinetics and measure properties such as the interfacial energy and diffusion constants. Experimental interfacial energies shall be compared to results from first-principles simulations.

We propose to continue our efforts in understanding how metal alloys oxidize. Our work published to date[48] emphasized imaging what actually happens as a thin, relatively uniform alumina film is grown using a literature "recipe."[46,47] Greatly different results are found under different oxidation conditions, however. When the NiAl (110) surface is exposed to oxygen above about 600°C, rod-shaped islands of crystalline oxide form (see Fig. 17 and Movie 6 on accompanying CD). We believe that these rods are spinel, $NiAl_2O_4$.[37] The spinel rods can extend for several microns in length along the substrate's [001] direction (panel b). The rods can both grow and shrink by addition and subtraction, respectively, at their ends. This one-dimensional behavior leads to surprising dynamics.[64] For example, addition at one end and removal at the other end can cause the rods to translate across the surface. A rod can also shrink and totally vanish. In addition, when two rods move close to one another, one rod can grow at the expense of the adjacent rod. Importantly, we also observe (panel c) that the rod phase transforms into a completely different oxide phase, namely, the same gamma alumina (γ-Al_2O_3) phase produced following the literature "recipe."[46,47] This phase transformation appears to nucleate at steps on the NiAl surface. The γ-Al_2O_3 phase contains strain-relieving interfacial dislocations (panel d). We propose to quantify the rod motion as a function of pressure and temperature. From this, we hope to develop a detailed kinetic model of the anisotropic island growth that is able to evaluate the role of anisotropic misfit strain on the observed kinetics.

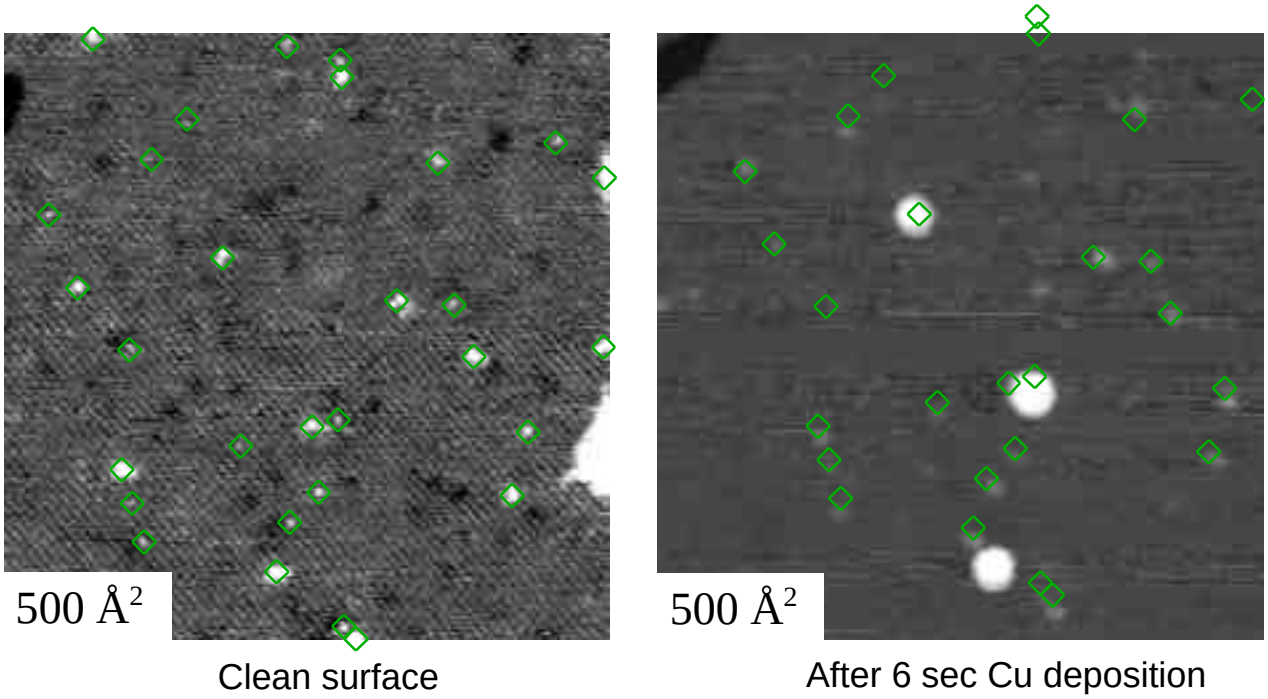

Fig. 13. Illustration of the ability to image the exact same region after depositing a metal on a ceramic surface. The STM images are of a TiO_2 (110) surface before (left panel) and after (right panel) Cu deposition. Two defect types are present on the clean surface -- "dark" defects and "bright" defects.[61] The latter are marked by the square symbols. The diagonal lines are the atomic rows on the clean surface.[65] In the field of view, three Cu islands have nucleated on or next to the bright defects. With further Cu deposition, islands nucleate away from any of the "bright" defects.

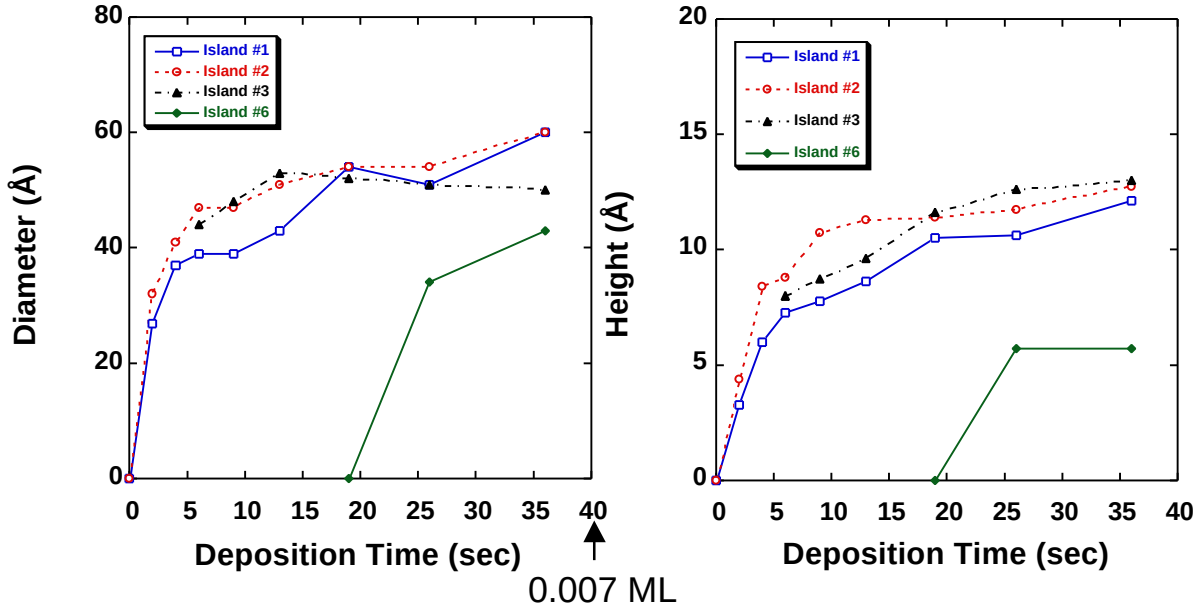

Fig. 14. The size of individual Cu islands on TiO_2 (110) as a function of dose. Even at the extremely low coverages, individual islands "self-limit" in both height and diameter. Islands 1-3 nucleated on or very near "bright" defects while the latter-born island 6 did not.

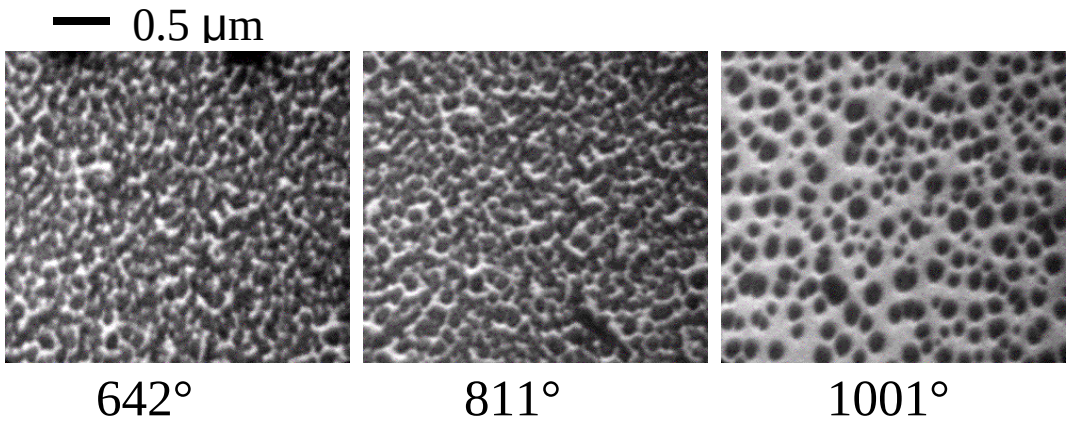

Fig. 15. Copper dewetting from the TiO_2 (110)-(1x1) surface. About 10Å of Cu was deposited at room temperature, giving a featureless, continuous film. At about 600°C, the Cu dewets the surface, forming discrete particles, which image dark compared to the brighter bare TiO_2 (110) substrate. The dewetting process is relatively isotropic, unlike on the reconstructed (1x2) surface (see Fig. 16).

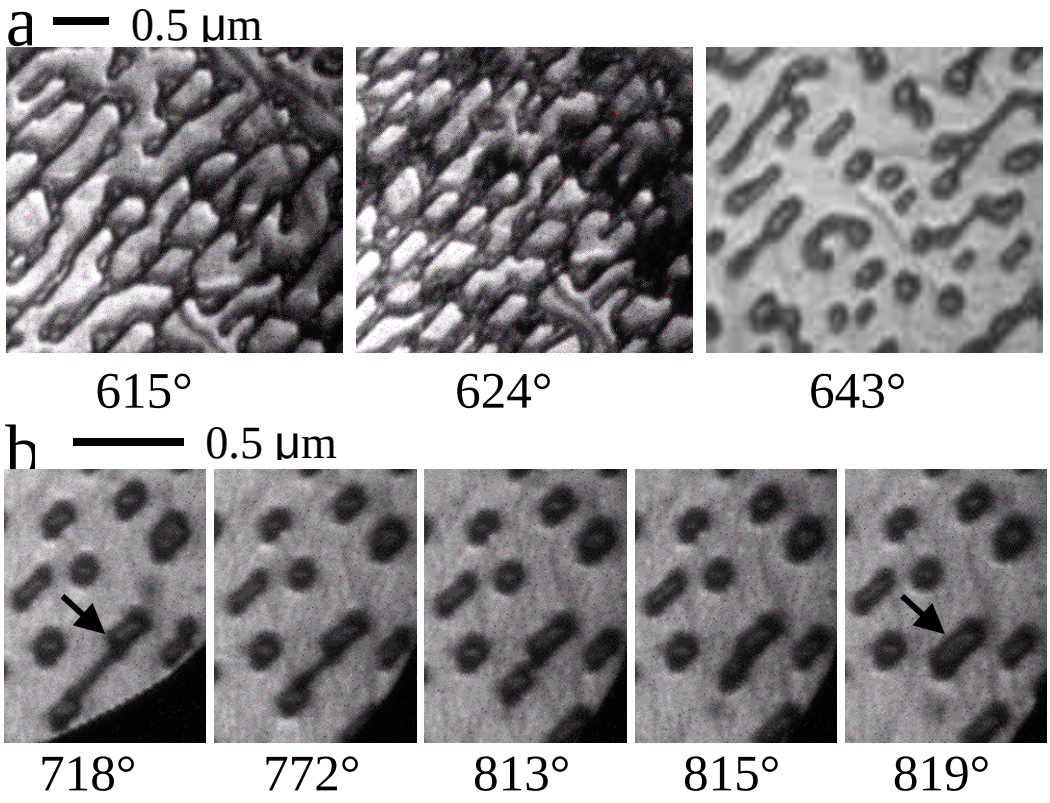

Fig. 16. Copper dewetting from the TiO_2 (110)-(1x2) surface. About 10Å of Cu was deposited at room temperature, giving a featureless, continuous film. On this reconstructed (oxygen-deficient) surface, the dewetting is highly anisotropic – the copper (dark features) forms very elongated structures. Part b shows an example of the curious mass transport that occurs. Two Cu particles are connected by a filament of Cu. The smaller particle is "reeled" into the larger particle marked by the arrow. This "liquid-like" behavior is occurring well below the melting point of Cu (1083°C). (See Movie 5 on accompanying CD.)

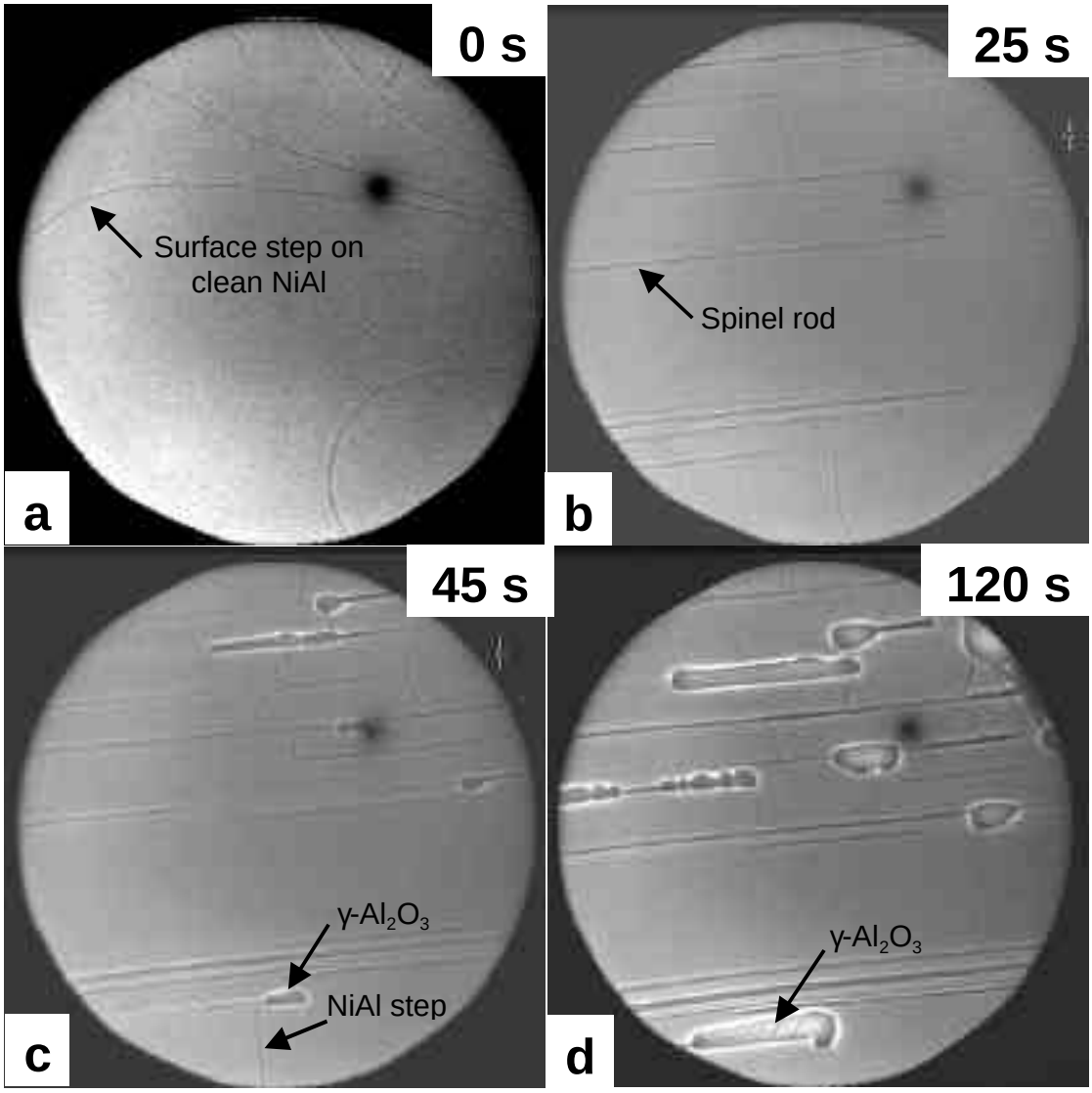

Fig. 17. Low-energy electron micrographs obtained during the oxidation of the NiAl (110) surface exposed to 10^{-7} torr of oxygen at 880°C. (See Movie 6 on accompanying CD.) Panel a shows the clean alloy surface before oxidation. The field of view is 5 μm. The dark lines are monoatomic steps on the alloy surface. Panel b, acquired 25 seconds after initiation of the oxygen exposure, has rod-shaped islands of crystalline oxide. These $NiAl_2O_4$ (spinel) islands exhibit fascinating dynamics, including translating along the surface. With time, some of the rods transform into "blob-shaped" islands (see panel c). Diffraction analysis establishes that these islands are γ−Al_2O_3. Thus, the initially formed spinel undergoes a transformation to a phase not containing nickel. The transformation appears to nucleate at NiAl steps. The γ−Al_2O_3 islands contain (see the zigzag structure of the island marked in panel d) linear features believed to be stress-relieving, interfacial dislocations.

Movie captions

Movie 1. A video (Quicktime format) example of what oscillating the sample temperature between 770 and 785°C does to surface morphology of NiAl (110). The imaged structure consists of a stack of islands, just like a tiered wedding cake. The dark lines in the low-energy electron microscopy (LEEM) images mark the surface steps, at which the height changes by one atomic layer between the atomically flat terraces. Thus the images are analogous to a topographic map with the steps corresponding to contours of constant elevation. The bar graphs show the sample temperature and area of the island topmost in the stack, respectively. As the temperature increases (decreases), the island area increases (decreases) by an amount strictly proportional to the step length of the island. These oscillations are superimposed upon a slow shrinkage of the island due to thermal smoothing. About half way through the movie, a dislocation (marked by the terminating surface step) moves into the field of view. While altering the local step configuration, the dislocation does not affect either the slow thermal smoothing or the size of the more rapid area changes. While the temperature oscillations of this example are quite small, larger temperature oscillations bring multiple layers to and from the surface. The field of view is 3.9 x 3.6 μm^2 and the elapsed time is 38 minutes.

Movie 2. A video (Quicktime format) example of isothermal island decay on the NiAl (110) surface at 985°C. Remarkable behavior is obvious in the movie -- all the islands are shrinking at once and at the same rate. Thus there is no evidence for mass being transported from the islands of highest curvature (the upper islands) to regions of lower curvature (the lower islands). While not shown, we also observe that adjacent islands of different size (radius of curvature) on the same terrace shrink at the same rate. That is, Ostwald ripening, where small (high chemical potential) islands shrink giving their mass to large (low chemical potential) islands, is also not occurring. The independence of the decay (smoothing) rate on the environment for both stacked and adjacent islands directly establishes that a surface diffusion process is not operative. The field of view is 5.8 x 5.8 μm^2 and the elapsed time is 6.7 minutes.

Movie 3. A video (Quicktime format) illustrating island growth on TiO_2 (110) upon exposure to 10^{-6} torr of O_2 at elevated temperature. (See Fig. 11.) The field of view is 5 μm. The dark lines mark the surface steps. While the oxygen comes from the gas phase, the titanium comes from the bulk of the crystal.

Movie 4. A video (Quicktime format) illustrating how the (1x2) structure forms on the TiO_2 (110) surface when the temperature is lowered. (See Fig. 12.) The field of view is 5 μm. The images were obtained in bright field using an electron energy that gives a large contrast between the (1x1) and the (1x2) phases, with the latter phase appearing dark. As the temperature is lowered, the step marked retracts (i.e., the island shrinks). If the temperature is above some critical temperature, (1x1) phase is left in the region the step passes through. Below the composition-dependent critical temperature, however, the bulk cannot accommodate all the Ti liberated when the step retracts. Then Ti-rich (1x2) phase is left in the region the step passes through.

Movie 5. A video (Quicktime format) showing copper dewetting from the TiO_2 (110)-(1x2) surface. (See Fig. 16.) The field of view is 5 μm. About 10Å of Cu was deposited at room temperature, giving a featureless, continuous film. On this reconstructed (oxygen-deficient)

surface, the dewetting is highly anisotropic – the copper (dark features) forms very elongated structures.

Movie 6. A video (Quicktime format) showing low-energy electron micrographs obtained during the oxidation of the NiAl (110) surface exposed to 10^{-7} torr of oxygen at 880°C. (See Fig. 17.) The field of view is 5 μm. Initially, the sample is in vacuum and the curved lines are steps on the clean alloy surface. When the oxygen exposure begins, rod-shaped islands of crystalline oxide form. These $NiAl_2O_4$ (spinel) islands exhibit fascinating dynamics, including translating along the surface. With time, some of the rods transform into "blob-shaped" islands of γ–Al_2O_3. Thus, the initially formed spinel undergoes a transformation to a phase not containing nickel. The transformation appears to nucleate at NiAl steps. Toward the end of the video, the γ–Al_2O_3 island near the bottom develops a zigzag structure that is believed to be a stress-relieving, interfacial dislocation.

References

1. Narula, C. K., Allison, J. E., Bauer, D. R. & Gandhi, H. S. Materials chemistry issues related to advanced materials applications in the automotive industry. *Chemistry of Materials* **8**, 984-1003 (1996).
2. Nitta, A. Current status and future work in the development of advanced materials for gas turbine components used at very high temperatures. *Journal of the Japan Institute of Metals* **64**, 958-964 (2000).
3. Satterfield, C. N. *Heterogeneous Catalysis in Industrial Practice* (Kreiger Publishing, Malabar, 1996).
4. Wang, C. C., Akbar, S. A. & Madou, M. J. Ceramic based resistive sensors. *Journal of Electroceramics* **2**, 273-282 (1998).
5. Tressler, J. F., Alkoy, S. & Newnham, R. E. Piezoelectric sensors and sensor materials. *Journal of Electroceramics* **2**, 257-272 (1998).
6. Zakrzewska, K. Mixed oxides as gas sensors. *Thin Solid Films* **391**, 229-238 (2001).
7. Donald, I. W., Metcalfe, B. L. & Taylor, R. N. J. The immobilization of high level radioactive wastes using ceramics and glasses. *Journal of Materials Science* **32**, 5851-5887 (1997).
8. Fernie, J. A. & Hanson, W. B. Best practice for producing ceramic-metal bonds. *Industrial Ceramics* **19**, 172-175 (1999).
9. Troczynski, T., Cockcroft, S. & Wong, H. Thermal barrier coatings for heat engines. *Key Engineering Materials* **122-**, 451-462 (1996).
10. Breval, E. Synthesis Routes to Metal-Matrix Composites with Specific Properties: A Review. *Composites Engineering* **5**, 1127-1133 (1995).
11. Howe, J. M. Bonding, Structure, and Properties of Metal-Ceramic Interfaces 1. Chemical Bonding, Chemical-Reaction, and Interfacial Structure. *International Materials Reviews* **38**, 233-256 (1993).
12. Tong, H. M. Microelectronics Packaging: Present and Future. *Materials Chemistry and Physics* **40**, 147-161 (1995).
13. Frankel, G. S. Pitting corrosion of metals: A review of the critical factors. *Journal of the Electrochemical Society* **145**, 2186-2198 (1998).
14. Galasso, F. S. *Structure and Properties of Inorganic Solids* (Pergamon Press, Oxford, 1970).
15. Henrich, V. E. & Cox, P. A. *The Surface Science of Metal Oxides* (Cambridge University Press, Cambridge, 1996).
16. Toofan, J. & Watson, P. R. The termination of the alpha-Al_2O_3 (0001) surface: a LEED crystallography determination. *Surface Science* **401**, 162-172 (1998).
17. Ahn, J. & Rabalais, J. W. Composition and structure of the Al_2O_3 {0001}-(1x1) surface. *Surface Science* **388**, 121-131 (1997).
18. Guénard, P., Renaud, G., Barbier, A. & Gautier-Soyer, M. Determination of the alpha-Al_2O_3(0001) surface relaxation and termination by measurements of crystal truncation rods. *Surface Review and Letters* **5**, 321-324 (1998).
19. Walters, C. F., McCarty, K. F., Soares, E. A. & Van Hove, M. A. The surface structure of alpha-Al_2O_3 determined by low-energy electron diffraction: aluminum termination and evidence for anomolously large thermal vibrations. *Surface Science* **464**, L732-L738 (2000).
20. Williams, E. D. & Bartelt, N. C. Thermodynamics of Surface-Morphology. *Science* **251**, 393-400 (1991).
21. Chiang, Y.-T., Birnie, D. & Kingery, W. D. *Physical Ceramics* (John Wiley, New York, 1997).
22. Herring, C. in *Structure and Properties of Solid Surfaces* (ed. Smith, C. S.) (Univ. of Chicago Press, 1952).

23. Mullins, W. W. Flattening of a nearly plane solid surface due to capillarity. *Journal of Applied Physics* **30**, 77-83 (1959).
24. Millot, F. et al. High-Temperature Nonstoichiometric Rutile TiO_{2-x}. *Progress in Solid State Chemistry* **17**, 263-293 (1987).
25. Finnis, M. W. The theory of metal-ceramic interfaces. *Journal of Physics-Condensed Matter* **8**, 5811-5836 (1996).
26. Ernst, F. Metal-Oxide Interfaces. *Materials Science & Engineering R-Reports* **14**, 97-156 (1995).
27. Bogicevic, A. & Jennison, D. R. Variations in the nature of metal adsorption on ultrathin Al_2O_3 films. *Physical Review Letters* **82**, 4050-4053 (1999).
28. Thompson, C. V. Structure evolution during processing of polycrystalline films. *Annual Review of Materials Science* **30**, 159-190 (2000).
29. Howe, J. M. Bonding, Structure, and Properties of Metal-Ceramic Interfaces 2. Interface Fracture-Behavior and Property Measurement. *International Materials Reviews* **38**, 257-271 (1993).
30. Barbieri, A., Weiss, W., Van Hove, M. A. & Somorjai, G. A. Magnetite Fe_3O_4(111): Surface-Structure By LEED Crystallography and Energetics. *Surface Science* **302**, 259-279 (1994).
31. Bauer, E. Low-energy-electron microscopy. *Reports on Progress in Physics* **57**, 895-938 (1994).
32. McCarty, K. F., Nobel, J. A. & Bartelt, N. C. Vacancies in solids and the stability of surface morphology. *Nature* **412**, 622 (2001).
33. Hansen, K. H. et al. Palladium nanocrystals on Al_2O_3: Structure and adhesion energy. *Physical Review Letters* **83**, 4120-4123 (1999).
34. Hwang, R. Q. & Bartelt, M. C. Scanning tunneling microscopy studies of metal on metal epitaxy. *Chemical Reviews* **97**, 1063-1082 (1997).
35. Campbell, C. T. Ultrathin metal films and particles on oxide surface: structural, electronic and chemisorptive properties. *Surface Science Reports* **27**, 1-111 (1997).
36. Franchy, R. Growth of thin, crystalline oxide, nitride, and oxynitride films on metal and metal alloy surfaces. *Surface Science Reports* **38**, 199-294 (2000).
37. Doychak, J., Smialek, J. L. & Mitchell, T. E. Transient Oxidation of Single-Crystal Beta-NiAl. *Metallurgical Transactions A: Physical Metallurgy and Materials Science* **20**, 499-518 (1989).
38. Lozovoi, A. Y., Alavi, A. & Finnis, M. W. Surface stoichiometry and the initial oxidation of NiAl(110). *Physical Review Letters* **85**, 610-613 (2000).
39. Chen, D. A., Bartelt, M. C., Hwang, R. Q. & McCarty, K. F. Self-Limiting Growth of Copper Islands on TiO_2 (110)-(1x1). *Surfuce Science* **450**, 78 (2000).
40. Chen, D. A., Bartelt, M. C., Seutter, S. M. & McCarty, K. F. Small, uniform, and thermally stable silver particles on TiO_2(110)-(1x1). *Surface Science* **464**, L708-L714 (2000).
41. Hart (Ed.), L. D. *Alumina chemical science and technology handbook* (ed. Hart, L. D.) (American Ceramic Society Inc., Westerville, OH, 1990).
42. Soares, E. A., Van Hove, M. A. & Walters, C. F. The Structure of the α-Al_2O_3 (0001) Surface from Low-Energy Electron Diffraction: Al Termination and Evidence for Anomolously Large Thermal Vibrations. *Physical Review B-Condensed Matter* , submitted (2001).
43. Verdozzi, C., Jennison, D. R., Schultz, P. A. & Sears, M. P. Sapphire (0001) surface: clean and with d-metal overlayers. *Physical Review Letters* **82**, 799-802 (1999).
44. Ångström, A. J. New method of determining the thermal conductibility of bodies. *Philosophical Magazine* **25**, 130-143 (1863).
45. Bradley, A. J. & Taylor, A. An X-ray analysis of the nickel-aluminium system. *Proceedings of the Royal Society* **A159**, 56-72 (1937).

46. Jaeger, R. M. et al. Formation of a Well-Ordered Aluminum-Oxide Overlayer by Oxidation of NiAl(110). *Surface Science* **259**, 235-252 (1991).
47. Libuda, J. et al. Structure and Defects of an Ordered Alumina Film on NiAl(110). *Surface Science* **318**, 61-73 (1994).
48. McCarty, K. F. Imaging the crystallization and growth of oxide domains on the NiAl(110) surface. *Surface Science* **474**, L165-L172 (2001).
49. Jeong, H. C. & Williams, E. D. Steps on surfaces: experiment and theory. *Surface Science Reports* **34**, 175-294 (1999).
50. Kitazawa, K., Kuriyama, T., Fueki, K. & Mukaibo, T. Determination of Mass-Transport Mechanism of Rutile by Sinusoidal Profile Decay Method. *Journal of the American Ceramic Society* **60**, 363-366 (1977).
51. Henderson, M. A. Surface perspective on self-diffusion in rutile TiO_2. *Surface Science* **419**, 174-187 (1999).
52. Li, M. et al. Oxygen-induced restructuring of the TiO_2(110) surface: a comprehensive study. *Surface Science* **437**, 173-190 (1999).
53. Matzke, H. in *Nonstoichioemtric Oxides* (ed. Sørensen, O. T.) (Acedemic Press, New York, 1981).
54. Dieckmann, R. Point defects and transport in non-stoichiometric oxides: Solved and unsolved problems. *Journal of Physics and Chemistry of Solids* **59**, 507-525 (1998).
55. Asari, E. & Souda, R. Atomic structure of TiO_2(110)-p(1x2) and p(1x3) surfaces studied by impact collision ion-scattering spectroscopy. *Physical Review B-Condensed Matter* **60**, 10719-10722 (1999).
56. Bennett, R. A., Stone, P., Price, N. J. & Bowker, M. Two (1 x 2) reconstructions of TiO_2(110): Surface rearrangement and reactivity studied using elevated temperature scanning tunneling microscopy. *Physical Review Letters* **82**, 3831-3834 (1999).
57. Gan, S., Liang, Y. & Baer, D. R. Interplay between step anisotropy and surface phase transformation on TiO_2(110). *Physical Review B* **63**, 121401 (2001).
58. Onishi, H., Fukui, K. & Iwasawa, Y. Atomic-Scale Surface-Structures of TiO_2 (110) Determined by Scanning-Tunneling-Microscopy: A New Surface-Limited Phase of Titanium-Oxide. *Bulletin of the Chemical Society of Japan* **68**, 2447-2458 (1995).
59. Pang, C. L. et al. Added row model of TiO_2(110)1x2. *Physical Review B-Condensed Matter* **58**, 1586-1589 (1998).
60. Bartelt, M. C., Schmid, A. K., Evans, J. W. & Hwang, R. Q. Island size and environment dependence of adatom capture: Cu/Co islands on Ru(0001). *Physical Review Letters* **81**, 1901-1904 (1998).
61. Diebold, U. et al. Intrinsic defects on a TiO_2(110)(1x1) surface and their reaction with oxygen: a scanning tunneling microscopy study. *Surfuce Science* **411**, 135-153 (1998).
62. Zhang, L., Cosandey, F., Persaud, R. & Madey, T. E. Initial growth and morphology of thin Au films on TiO_2(110). *Surface Science* **439**, 73-85 (1999).
63. Dulub, O., Hebenstreit, W. & Diebold, U. Imaging cluster surfaces with atomic resolution: The strong metal-support interaction state of Pt supported on TiO_2(110). *Physical Review Letters* **84**, 3646-3649 (2000).
64. Koh, S. J. & Ehrlich, G. Stochastic ripening of one-dimensional nanostructures. *Physical Review B* **62**, 10645-10648 (2000).
65. Diebold, U., Anderson, J. F., Ng, K. O. & Vanderbilt, D. Evidence For the Tunneling Site On Transition-Metal Oxides: TiO_2(110). *Physical Review Letters* **77**, 1322-1325 (1996).